8-2020

# A Data-Driven Regional Model of Stomatal Conductance for Kruger National Park

Rebecca L. Tobin
*Utah State University*

A DATA-DRIVEN REGIONAL MODEL OF STOMATAL CONDUCTANCE FOR

KRUGER NATIONAL PARK

by

Rebecca L. Tobin

A thesis submitted in partial fulfillment
of the requirements for the degree

of

MASTER OF SCIENCE

in

Ecology

Approved:

| | |
|---|---|
| Andrew Kulmatiski, Ph.D.<br>Major Professor | Karen H. Beard, Ph.D.<br>Committee Member |
| Bruce Bugbee, Ph.D.<br>Committee Member | Janis L. Boettinger, Ph.D.<br>Acting Vice Provost of Graduate Studies |

UTAH STATE UNIVERSITY
Logan, Utah

2020

# ABSTRACT

A Data-driven Regional Model of Stomatal Conductance for Kruger National Park

by

Rebecca Tobin, Master of Science

Utah State University, 2020

Major Professor: Dr. Andrew Kulmatiski
Program: Ecology

The basic drivers of stomatal conductance ($g_s$) are well understood at the leaf level under controlled conditions, but it has been difficult to extrapolate laboratory principals to plant communities. Here we estimate and model landscape-level $g_s$ from a dataset with over 8,000 $g_s$ measurements made over five years from four study sites in Kruger National Park, South Africa. Sites represented a wide range of precipitation (450-750 mm mean annual precipitation) and soil types (sand and clay). Measurements were used in a machine-learning (Random Forest) model to assess the effects of plant functional type (grass or woody), species, vapor pressure deficit, soil moisture, shortwave radiation, wind speed, atmospheric [$CO_2$], time-of-season, soil type, and precipitation on $g_s$. Both plant functional type and species had large effects on $g_s$. Among environmental variables, shallow soil moisture had the greatest effect on $g_s$ for both grasses and woody plants. Soil type had the smallest effect on $g_s$ for both plant functional types. The effect of environment differed between grasses and woody plants. When the models were used with observed environmental data from several growing seasons, mean daytime $g_s$ was estimated as 67 and 158 mmol $m^{-2}$ $sec^{-1}$ for grasses and woody plants, respectively. While laboratory-based models emphasize the role of leaf-level environmental parameters, this dataset highlights the role of species identity and soil moisture as major drivers of $g_s$ at the landscape scale. Results also show a large amount of landscape-scale variability in $g_s$ that remains to be explained.

(47 pages)

# PUBLIC ABSTRACT

A Data-driven Regional Model of Stomatal Conductance for Kruger National Park

Rebecca Tobin

Stomata are the gateway between the lithosphere, the biosphere, and the atmosphere. Because of photosynthesis, plants inevitably lose water through their stomata. The rate at which water moves through stomata is stomatal conductance. As stomatal conductance increases, the rate of $CO_2$ assimilation increases, therefore, plants must reach a balance between acquiring $CO_2$ and losing $H_2O$. Plants achieve this balance by adjusting stomatal aperture. Therefore, modeling stomatal conductance is important to global circulation models and land surface models, as well as for predicting how changing climate conditions affect water use efficiency and plant productivity, and has implications for agriculture and natural resource management.

Here a large dataset of field measurements was used to describe stomatal conductance for Kruger National Park, South Africa and develop statistical models of landscape-level stomatal conductance. Then models were used to estimate stomatal conductance across the region over several growing seasons. Over 8,000 measurements of stomatal conductance were made in four sites that represented a range of precipitation regimes and soil types within Kruger National Park from 2007-2012. Known environmental drivers of stomatal conductance, such as soil moisture, temperature, and shortwave radiation, were also measured during this period.

Observed mean daytime stomatal conductance for the park was $75 \pm 1$ and $155 \pm 2$ mmol $m^{-2}$ $sec^{1}$ for grasses and woody plants, respectively. When statistical models were

used to produce three years of continuous estimates of $g_s$ from environmental data, average daytime stomatal conductance was estimated as 67 and 158 mmol $m^{-2}$ $sec^{-1}$ for grasses and woody plants, respectively. The Random Forest statistical models that were used to produce continuous estimates of $g_s$ indicated that soil moisture, particularly at shallow depths, and plant species identity are primary drivers of landscape-scale stomatal conductance for Kruger National Park. However, results indicate that there is still a large amount of landscape-scale variability in stomatal conductance that the environmental drivers investigated here were unable to explain.

Results provide a rare example of landscape-level estimates of stomatal conductance based on direct measurements. The models give insight into the relative importance of environmental drivers and the nature of their effect on stomatal conductance in savanna ecosystems. Because the measurements were collected over a range of species and soil conditions, the models should provide inference for many deciduous, sub-tropical savannas of southern Africa.

# ACKNOWLEDGMENTS

This study would not have been possible without the cooperation of South African National Parks and Kruger National Park (project registration number 213896412). I would like to thank the Andrew Mellon Foundation, the Utah State University Agricultural Experiment Station, and the Office of Research and Graduate Studies for funding this project. Thank you to my major professor: Andrew Kulmatiski, my thesis committee: Karen H. Beard and Bruce Bugbee, and S. Durham and Thomas C. Edwards for assistance in statistical analyses and modeling. Thank you also to the field managers: M. Keretetse, S. Heath, L. Hierl, M. Cooper, and M. Mazzacavallo and the field/laboratory assitants: W. Sibuyi, R. Mashele, V. Sibuyi, and M. Rogers.

Rebecca Tobin

# CONTENTS

# LIST OF TABLES

LIST OF FIGURES

## INTRODUCTION

Because stomatal conductance ($g_s$) is a measure of gas exchange between plants and the atmosphere, $g_s$ is an important component of $CO_2$ and water cycles at both local and global scales[1–4]. Therefore, understanding the factors that determine $g_s$ is important for predicting small-scale processes such as plant productivity[1], species coexistence and crop water use[4] as well as large-scale processes, such as global $CO_2$ and energy budgets[2,5].

Models of $g_s$ are numerous, well-developed[1,3,6] and fall into three general categories: empirical, mechanistic, and optimization[3]. Empirical, or data-based, models describe the response of $g_s$ to environmental parameters, such as irradiance[1], temperature, vapor pressure deficit (VPD)[1,7], $CO_2$ concentration[6–8], water stress[1], and interactions among these drivers. Because many factors can affect gs, the majority of empirical approaches have been conducted in laboratory settings where the effect of individual factors can be tested. The empirical $g_s$ models developed by Jarvis[9] (including subsequent Jarvis-type models[6]) and Ball, Berry, and Woodrow[10] provide reasonable estimates of $g_s$ under laboratory conditions and some of the best estimates of gs under field conditions[3,11]. As a result, these models are widely-used in global circulation models, earth system models, and models of canopy-level processes[2,3]. However, due to the difficulty of measuring gs in the field[1], validation of model predictions remains limited[3,9,10]. Mechanistic approaches rely on models and tests of the role of specific mechanisms, but are often difficult to apply to the landscape-level[3,11]. Finally, optimization models seek to predict $g_s$ behavior according to the premise that $g_s$ is regulated to maximize photosynthesis and minimize water loss[2,3,5]. Although there can be computational difficulties in implementing optimization models[3], there have been recent efforts to incorporate $g_s$ optimization models into earth system models[2,5,12].

Developing $g_s$ models applicable on a landscape or global scale has proven difficult[1,2,13]. Due in part to technological limitations[1], $g_s$ datasets are rarely large enough to capture the variability in $g_s$ that occurs among species, within canopies, and over daily and seasonal time-scales in response to environmental drivers, such as soil moisture and VPD. As a result, response curves generated from limited observations may not be applicable across landscapes[14]. Savanna ecosystems pose a particular challenge because they include alternative dominant life forms: grasses and trees that can vary widely in both $g_s$ and their $g_s$ responses to environmental drivers. There remains, therefore, a need for both datasets and models of landscape-scale drivers of $g_s$ across growing seasons for this region.

The overarching goal of this study was to describe $g_s$ in the savanna ecosystems of the nearly 2 million ha Kruger National Park and surrounding ecosystems in South Africa. More specifically, the objectives were: 1) to develop a dataset large enough to describe $g_s$ for Kruger National Park, 2) to use the dataset to build a landscape-scale model of $g_s$ and 3) to use the model and observed environmental data to produce continuous estimates of $g_s$ across Kruger Park for three growing seasons. To capture landscape-scale variability in $g_s$, measurements were collected over five years in four sites that represent a wide range of abiotic and biotic conditions. A machine-learning approach (Random Forest, hereafter RF) was used to describe the effect of the following environmental parameters on $g_s$: soil moisture, VPD, shortwave radiation, wind speed, soil type, precipitation regime, time-of-season, time-of-day, atmospheric [$CO_2$], and species identity, on $g_s$. RF modeling has been shown to reveal nonlinear relationships and complex interactions in ecological data that may be missed by other statistical methods[15]. Because different species and functional groups are influenced by and respond differently to environmental conditions[16], separate RF models were developed and conducted for grasses and woody plants. The RF models that explained the greatest variance in the $g_s$ dataset were used with environmental data to produce continuous, three-year estimates of $g_s$ for each study site and the entire study area.

# METHODS

## *2.1 Study Site Information*

Research was conducted between 2007 and 2012 in four deciduous, subtropical savanna sites in Kruger National Park, South Africa: Letaba (-23°46'49.00" S, 31°31'16.19" E), Phalaborwa (-23°51'25.27" S, 31°14'12.75"E), Pretoriuskop (-25°12'21.68" S, 31°17'9.92" E), and Lower Sabie (-25°12'2.09" S, 31°54'27.25" E). The four sites were selected to provide broad inference to conditions on the landscape, and represented a two-by-two factorial combination of precipitation ("wet" or "dry") and soil texture ("sand" or "clay")(Table 1)[17,18]. Common grasses include *Bothriochloa radicans* (Lehm) A. Camus, *Setaria incrassate* (Hochst.) Hack. and *Urochloa mosambicensis* (Hack.) Dandy. Common woody plants include *Terminalia sericea* Burch. ex DC and the nitrogen-fixing *Colophospermum mopane* (Benth.) Leonard and *Dichrostachys cinerea* subsp. *africana* (Brenan & Brummitt)(Table 2).

Table 1. Precipitation regimes and soil types corresponding to the four study sites within Kruger National Park, South Africa[17,18].

| Site Name | Soil Type | Precipitation Regime |
|---|---|---|
| Letaba | Clay (calcareous shallow clay) | Dry (450 MAP) |
| Phalaborwa | Sand (coarse fersiallitic sand) | Dry (475 MAP) |
| Lower Sabie | Clay (pedocutanic clay) | Wet (730 MAP) |
| Pretoriuskop | Sand (coarse fersiallitic sand) | Wet (750 MAP) |

*2.2 Study Design*

***Stomatal conductance measurements:*** At each site, $g_s$ measurements were made across a roughly 4 ha sampling area that had been established for related research[19–21]. $g_s$ was measured using steady-state porometers (Decagon Devices, SC-1)[22], which take $g_s$ measurements in 30 seconds, allowing large sample sizes relative to null-balance porometers or dynamic porometers[23]. Measurements were made during six sampling campaigns that represented early, mid- and late-season sampling during each of two growing seasons at each site. Each sampling campaign included 2-3 days of sampling. To prevent biased sampling of certain samples (*i.e.*, plant species), measurements were made during either consistent cloud cover or clear skies. Sampling was intended to be as representative of landscape-level $g_s$ as possible, so samples were collected between sunrise and sunset, and were taken throughout the plant canopy[20,21,24]. For grasses, $g_s$ was measured from both abaxial and adaxial surfaces. For woody plants, $g_s$ was not detectable on adaxial surfaces and was not measured. Forbs were also sampled, although their relative abundance was small compared to grasses and woody plants. Each of roughly 10 dominant target species at a site was measured within 15-minute increments to control for environmental variability. The species, plant functional type, soil type (clay or sand) and precipitation regime (wet or dry) and time-of-season [early (November – December), middle (January – February) or late (March - April)] in which measurements were taken were recorded. Tree and shrub species were classified together as "woody" (Table 2).

Table 2. Species, plant functional type and sample sizes from each study site. LT = Letaba, LS = Lower Sabie, PB = Phalaborwa, PK = Pretoriuskop. Numbers in parentheses indicate sample size.

| Species | Code | Plant type | Sample Size by Site |
|---|---|---|---|
| *Acacia nigrescens* | ACAN | Woody | PB (33) LS (208) |
| *Lonchocarpus capassa* | APPL | Woody | PB (15) PK (3) LS (107) |
| *Bothriocloa radicans* | BRAR | Grass | LT (456) PB (12) LS (60) |
| *Combretum apiculatum* | COMA | Woody | LT (12) PB (102) |
| *Combretum imberbe* | COMI | Woody | PB (36) LS (68) |
| *Loudetia simplex* | CORU | Grass | PK (134) |
| *Dichrostachys cinerea* | DICH | Woody | PB (106) PK (749) LS (402) |
| *Grewia bicolour* | GREW | Woody | PB (12) LS (109) |
| *Sclerocarya birrea* | MARU | Woody | LT (2) PB (24) PK (148) LS (1) |
| *Colophospermum mopane* | MOPA | Woody | LT (843) PB (178) |
| *Panicum spp.* | PANI | Grass | LT (11) PB (71) LS (234) |
| *Terminalia sericea* | SCLE | Woody | PB (1) PK (797) |
| *Urochloa mosambicensis* | UROC | Grass | LT (25) PB (76) LS (245) |
| *Setaria incrassata* | VLEI | Grass | PK (458) |
| *Securinega virosa* | WHBE | Woody | PB (128) LS (298) |
| *Ximenia caffra* | XIME | Woody | PK (106) |

***Environmental parameters:*** Temperature, relative humidity (215L; Campbell Scientific, UT, USA), wind speed (014A cup anemometer; MetOne, OR, USA), total shortwave radiation (SP-110; Apogee Instruments, UT, USA), and precipitation (Texas Instruments TE-525; Texas Instruments, TX, USA) were recorded at each site on Campbell Scientific CR1000 dataloggers. Measurements were made at both “grass” (1 m) and “woody” (2 m) canopy heights, except at Pretoriuskop, where only 2 m heights were measured. Air temperature and relative humidity were used to calculate VPD using the following equations[25]:

$$e_s = 0.611^{\frac{17.27(T)}{T+237.3}}$$

$$e_a = \frac{RH}{100} x\ es$$

$$VPD = e_a - e_s$$

where $e_s$ is the saturation vapor pressure (kPa), $e_a$ is the actual vapor pressure (kPa), $T$ is the air temperature (°C), and $RH$ is the relative humidity (%). Atmospheric [$CO_2$] measurements were provided by a flux tower near Skukuza[26]. Heat dissipation sensors (229; Campbell Scientific, UT, USA) were used to produce a soil water potential "index" for 0-20 cm, 0-50 cm, 20-50 cm, and 50-150 cm depths for each site[21]. Each heat dissipation sensor was calibrated prior to installation by taking measurements from soil samples equilibrated to specific water potentials[21]. To preclude error associated with developing site-specific water potential curves, sensor-specific values of proportional temperature response were used as a soil moisture index[18,21,27].

### *2.3 Data Analyses and Statistics*

Simple means and errors of observed daytime $g_s$ by plant functional type for the entire dataset and by site are reported. Species with less than 100 measurements in the dataset were excluded (Table 2). One-way analysis of variance was used to test for differences in mean $g_s$ values among sites for each plant functional type[28]. To meet assumptions of normality, $g_s$ values were log-transformed. Because sample sizes differed among sites, Type III sum of squares were used. Pairwise comparisons were examined using the Tukey test[29].

***Random Forest modeling:*** Random Forest modeling was used to describe the relationship between environmental parameters and $g_s$ and to build a predictive model of landscape-scale $g_s$[15]. In RF, a “forest” of regression trees is fit to a training dataset (approximately two-thirds of the sample data). The trees are then used to predict the out-of-bag data (*i.e.* the sample data not included in the training dataset) and the predictions from all trees are combined, giving a cross-validated measure of the accuracy of the model[15,30]. The relative importance of predictors within the RF models was compared and $g_s$-predictor relationships were visualized. The RF models that explained the most variance were used to estimate $g_s$ using environmental data from 3-4 growing seasons. Model estimates were generated by plant functional type. Statistical analyses were performed in RStudio[31]. All RF models and predictions were developed using the R package “randomForestSRC”[32] and all model visualizations were created using the “ggRandomForests” package[33].

For RF modeling, $g_s$ measurements were paired with meteorological and soil measurements from the closest recorded timestep. Missing meteorological and soil data were interpolated where possible by correlating and adjusting data from the nearest weather station using a simple linear equation (y = mx + b, where y is the adjusted measurement and x is the original measurement). To test for potential lag effects in the response of $g_s$ to environmental conditions, the three-hour (3-hour) averages of air temperature, relative humidity, VPD, wind speed, and shortwave radiation, the 3-hour, 24-hour, and seven-day (7-day) averages of each soil moisture depth, and the 24-hour sum of precipitation were calculated.

Although highly-correlated predictors do not affect RF variable importance[15], to simplify interpretation of variable relationships, correlation matrices for groups of related predictor variables were used to test multicollinearity[15]. Air temperature, relative humidity, VPD, shortwave radiation, wind speed, precipitation, and soil moisture depths were evaluated. Because data for numerical predictor variables were not all distributed normally, Spearman correlation was used[34]. Where two predictors were highly correlated (correlation > ± 0.7), the predictor with the greatest "adjusted squared deviance explained" by a generalized linear model (GLMs; linear + quadratic, family = Gaussian) was used in the RF model[15]. When highly-correlated predictors explained similar (difference of less than 2 %) amounts of variance in $g_s$, separate RF models were created to test the amount of variance explained with different combinations of predictors. The "best" RF models were selected based on the amount of variance in the dataset they explained. Categorical predictors were plant functional type, species, time-of-season, precipitation regime, and soil type.

Variable importance (VIMP) within the RF model was determined and visualized using the ggRandomForests package[33]. Each variable was randomly permutated and the prediction error calculated using the out-of-bag data[15]. The VIMP value for each variable is the difference between the out-of-bag prediction error of the observed and permutated variables. Large VIMP values indicate that specifying the variables incorrectly increases prediction error; therefore, variables with large VIMP values are more important.

Negative VIMP values indicate that the randomly permutated variable was a better predictor than the observed variable[33].

Relationships between $g_s$ and its environmental parameters were characterized with risk-adjusted partial dependence plots created using the "ggRandomForests" package[33]. Partial dependence refers to the dependence of the response variable, in this case $g_s$, on one predictor variable[15]. The plots were created by averaging the effects of the other predictors and predicting how the response variable changes with the predictor of interest alone[15]. Partial dependence of categorical variables was analyzed by comparing the mean predicted $g_s$ of each level of the variable. To avoid confusion with model predictions made with new data, "estimated" was used to describe partial dependence predictions.

$g_s$ sampling was designed to produce a representative sample of $g_s$ on the landscape. However, because sampling was difficult to perform at sunrise and sunset for safety reasons (dangerous animals occupy the areas) and during fluctuating cloud conditions and during rain, the models were used to produce continuous estimates of $g_s$ across three growing seasons.  This approach produced estimates that were not biased by a low number of samples at sunrise and sunset. Model predictions of $g_s$ were generated using data from three growing seasons from each study site (2009 – 2012). The data were collected and prepared using the same instrumentation and methods as the data used to build the RF models. The data were then run through the RF models using the "predict" function in the "randomForestSRC" package[32]. Model predictions were generated separately for each study species. The modeled $g_s$ values were averaged by plant functional type for each study site and for the entire park.

# RESULTS

## *3.1 Observed $g_s$*

Over the five years of the study, 8510 $g_s$ measurements were made. Mean observed daytime $g_s$ was 74 ± 1 mmol m$^{-2}$ s$^{-1}$ for grasses, 155 ± 2 mmol m$^{-2}$ s$^{-1}$ for woody plants, and 142 ± 5 mmol m$^{-2}$ s$^{-1}$ for forbs. The total cover and sample size for forbs was small (580) relative to grasses and woody plants (2662 and 4962, respectively) and was not included in further analyses. Mean observed $g_s$ was greater in the wet/clay site than the other sites for both grasses ($F = 28.399$, $p < 0.001$) and woody plants ($F = 77.298$, $p < 0.001$).

## *3.2 Random Forest*

Across both plant functional types, the best RF model explained 58 % of variance and included, in descending order of importance: species, 24-hour shallow soil moisture, 24-hour deep soil moisture, 3-hour shortwave radiation, 3-hour VPD, 3-hour wind speed, atmospheric [$CO_2$], time-of-season, time-of-day, precipitation regime, and soil type. When species was replaced with plant functional type as a predictor, the percent variance explained by the model decreased to 51 %. When neither species nor plant functional type was included in the model, percent variance explained decreased to 43 %. However, because it is reasonable to expect that grasses and woody plants may respond differently to environmental drivers[16], and because savannas show wide variations in woody plant cover[17], separate models were created for each plant functional type group. Percent variance explained for the grass dataset with and without species was 21 % and 20 %, respectively. Percent variance explained for the woody $g_s$ dataset with and without species was 54 % and 45 %, respectively.

For both plant functional types, shallow (0-20 cm) soil moisture and soil type were the most and least important predictors of $g_s$, respectively (Fig. 1). The remaining variables differed in importance between grasses and woody plants. For grasses, in descending order of importance: VPD, atmospheric [$CO_2$], time-of-day, deep (50-150cm) soil moisture, time-of-season, wind speed, shortwave, radiation, species, precipitation regime, and soil type explained variance in $g_s$ (Fig. 1). For woody plants, in descending order of importance: shortwave radiation, precipitation regime, species, atmospheric [$CO_2$], VPD, wind speed, deep (50-150cm) soil moisture, time-of-season, time-of-day, and soil type explained variance in $g_s$ (Fig. 1).

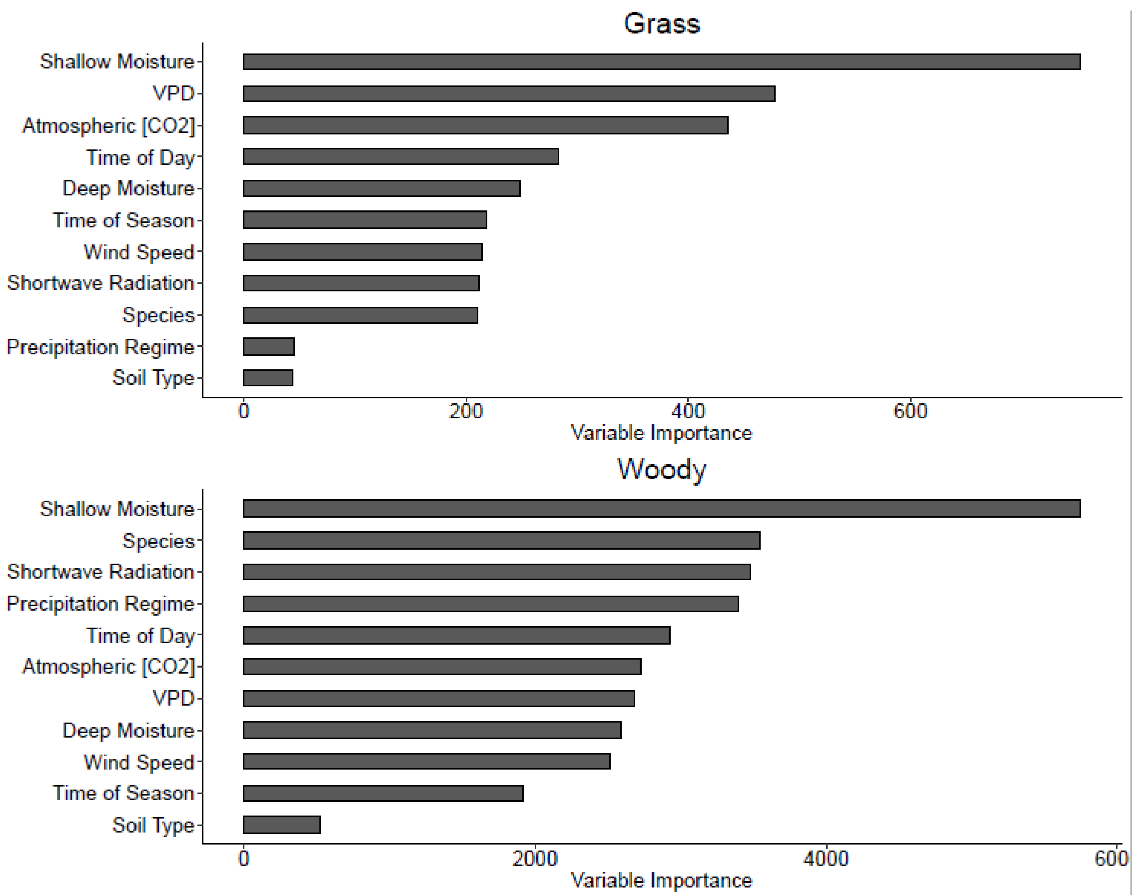


Fig 1. Variable importance in random forest models of stomatal conductance for grasses and woody plants. Variable importance is the difference in prediction error before and after a predictor variable is randomly permutated. Large variable importance values indicate that specifying the variables incorrectly increases prediction error.

Estimated grass $g_s$ increased with shallow soil moisture, decreased with VPD, and decreased with shortwave radiation beyond 1250 $\mu$mol m$^{-2}$ s$^{-1}$ (Fig. 2). Estimated woody $g_s$ increased with soil moisture, both shallow and deep, showed a hump-shaped response to VPD that peaked near 1 kPa, and showed a hump-shaped response to shortwave radiation, peaking near 500 $\mu$mol m$^{-2}$ s$^{-1}$. Both grass and woody plant estimated $g_s$ increased with increasing atmospheric [$CO_2$]. Wind speed did not exhibit a clear relationship with grass or woody plant $g_s$. Estimated $g_s$ also differed among categorical variable levels. Mean estimated grass $g_s$ decreased (3 %) over the growing season. Mean estimated $g_s$ for woody plants peaked mid-season. Mean estimated grass $g_s$ differed by less than 1 % between wet sites and dry sites and clay sites and sand sites (Fig. 3). Mean estimated woody plant $g_s$ was 16 % greater in wet sites than dry sites and 1.5 % greater in clay sites than sand sites (Fig. 3).

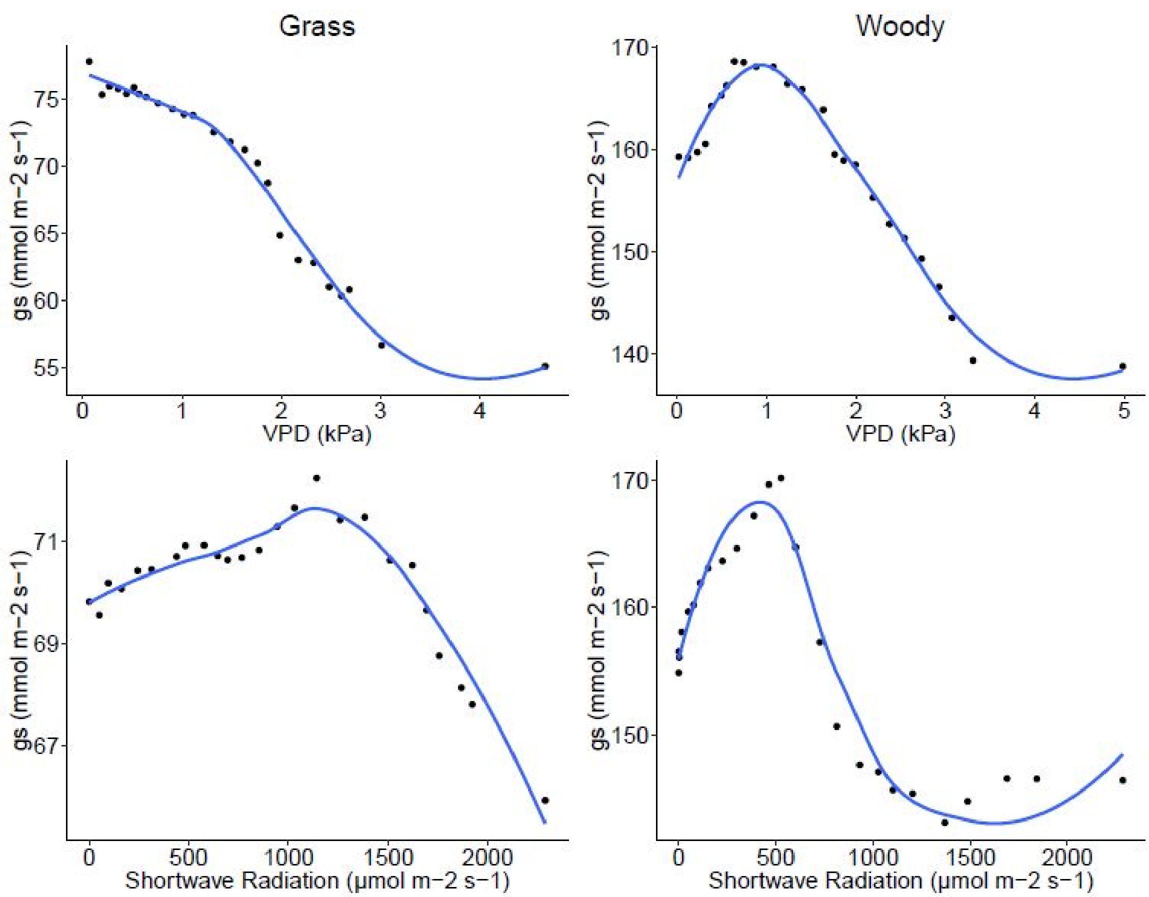


Fig 2. Partial dependence plots for VPD and shortwave radiation for grasses and woody plants. The top panels show estimated grass and woody plant gs as a function of VPD**.** The bottom panels show estimated grass and woody plant gs as a function of shortwave radiation. Partial dependence is determined by averaging the effects of the other predictors and predicting how the response variable changes with the predictor of interest alone.

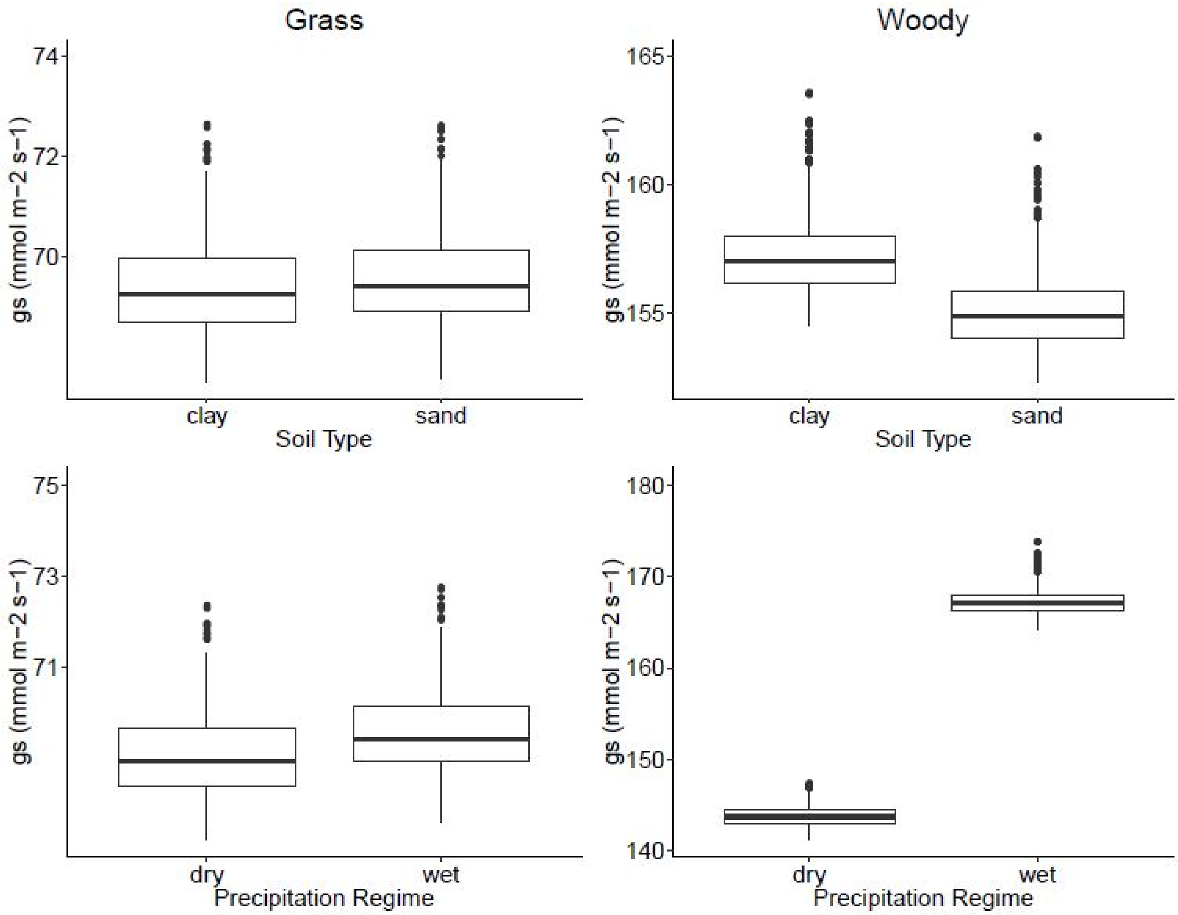


Fig 3. Partial dependence plots for soil type and precipitation regime. The top panels show estimated grass and woody plant $g_s$ as a function of soil type. The bottom panels show estimated grass and woody plant $g_s$ as a function of precipitation regime. Partial dependence is determined by averaging the effects of the other predictors and predicting how the response variable changes with the predictor of interest alone.

*3.3 Model Predictions of $g_s$*

When predicted by parameterizing our model with three years of observed environmental data, mean daytime $g_s$ across the four study sites was 67 and 158 mmol $m^{-2}$ $s^{-1}$ for grasses and woody plants, respectively. The wet/sand site had the greatest predicted daytime $g_s$ for both grasses and woody plants (Fig. 4). Mean predicted daytime $g_s$ was 14 % - 24 % and 66 % - 92 % greater in the wet/sand site than other sites for grasses and trees, respectively. Mean predicted daytime $g_s$ differed by less than 10 % between the dry/clay and dry/sand sites for both grasses and woody plants. Mean predicted daytime $g_s$ differed between species (Fig. 5), although it should be noted that species were not evenly distributed across the abiotic conditions of the park. Predicted $g_s$ for grasses and woody plants decreased to a peak mid-morning before decreasing until sunset (Fig. 6). In general, predicted $g_s$ peaked mid-growing season for both grasses and woody plants.

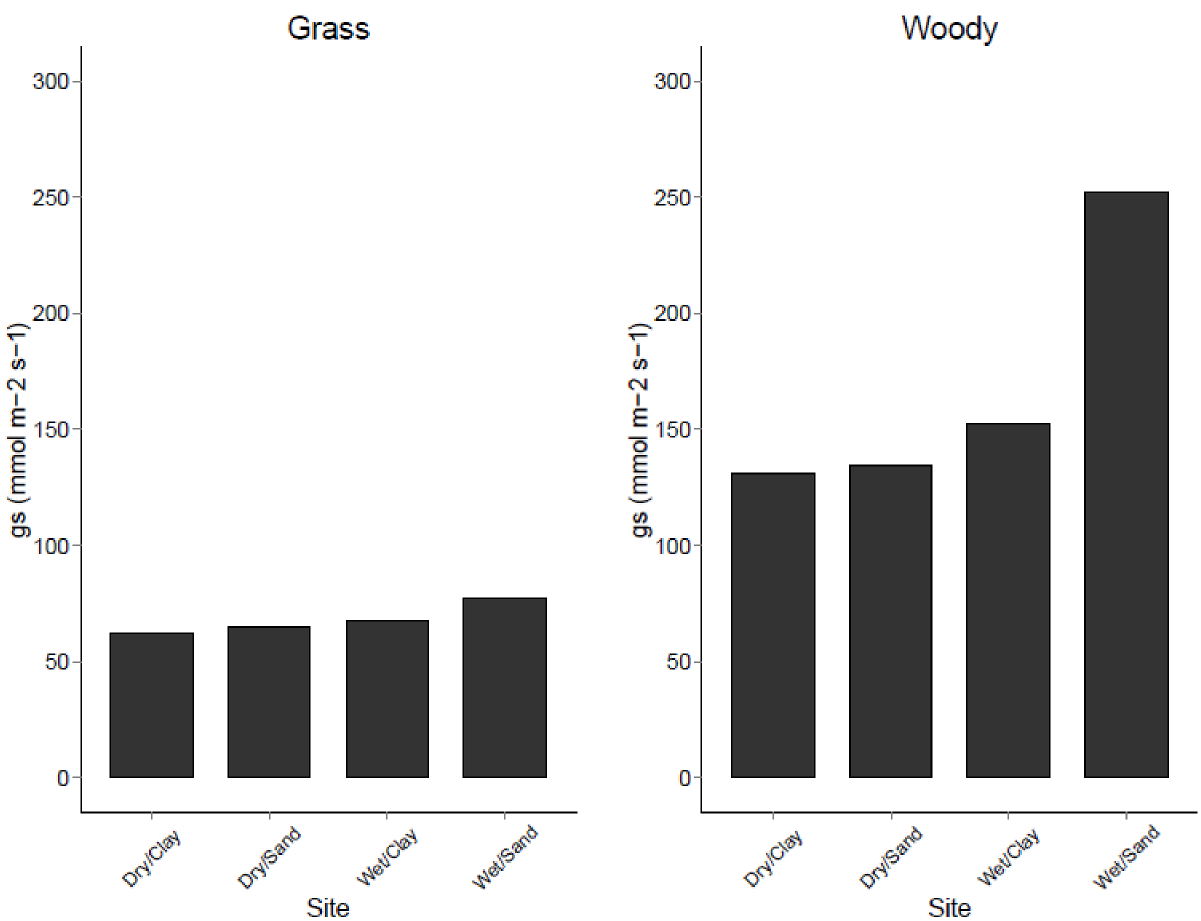


Fig 4. Mean modeled daily $g_s$ for each study site. Modeled daytime $g_s$ was greatest for the wet/sand site for both grasses and woody plants. $g_s$ differed by less than 10 % between the dry/clay and dry/sand sites for both grasses and woody plants.

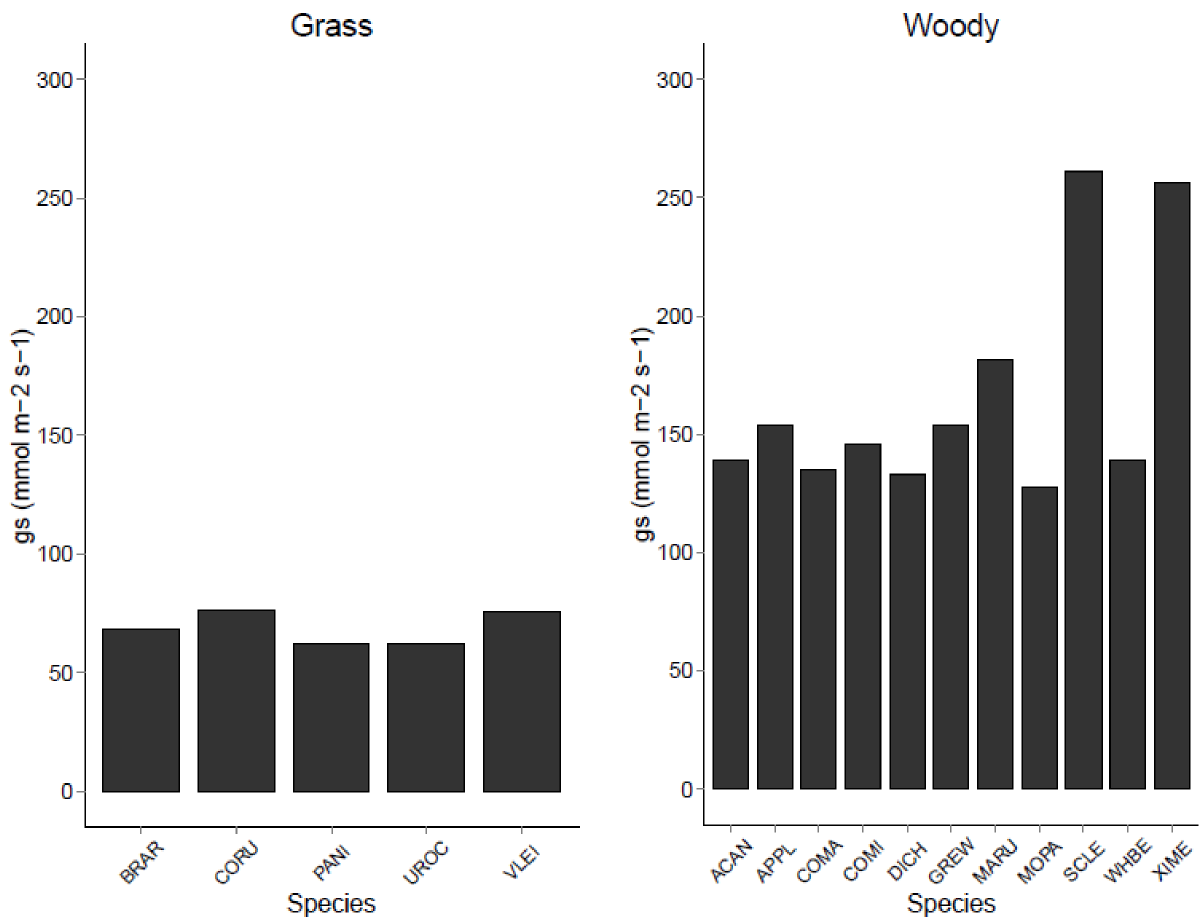


Fig 5. Mean modeled daytime $g_s$ for each species. BRAR = *Bothriochloa radicans*, CORU = *Loudetia simplex*, PANI = *Panicum spp.*, UROC = *Urochloa mosambicensis*, VLEI = *Setaria incrassata*, ACAN = *Acacia nigrescens* APPL = *Lonchocarpus capassa*, COMA = *Combretum apiculatum*, COMI = *Combretum imberbe*, DICH = *Dichrostachus cinerea*, GREW = *Grewia bicolour*, MARU = *Sclerocarya birrea*, SCLE = *Terminalia sericea*, WHBE = *Securinega virosa*, XIME = *Ximenia caffra*.

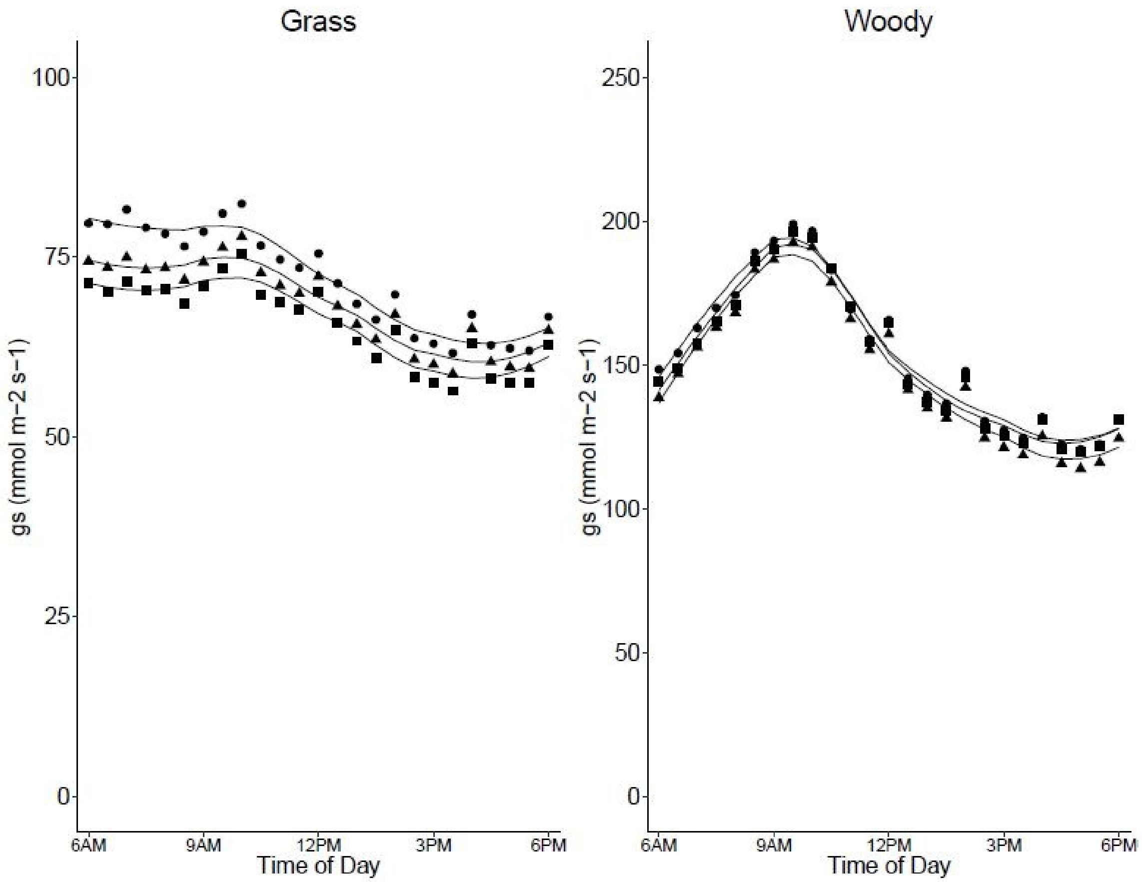


Fig 6. Modeled daily $g_s$ for grasses and woody plants at the dry/sand site. The shape of the points indicates the species. In the grass panel: circles for *Bothriochloa radicans*, triangles for *Panicum* spp., and squares for *Urochloa mosambicensis*. In the woody panel: circles for *Acacia nigrescens*, triangles for *Dichrostachys cinerea*, and squares for *Securinega virosa*. Model predictions were averaged for each timestep and mid-season values are shown.

# DISCUSSION

Using a large, field-based dataset, our results highlighted plant identity (functional type or species) and shallow soil moisture as primary drivers of $g_s$ across the sub-tropical savanna landscape of Kruger National Park. These results stand in contrast to a large body of laboratory-based research that has emphasized the role of environmental variables such as temperature[3,35,36], VPD[35,37,38], solar radiation[3,35,37], and atmospheric $[CO_2]$[35,39,40] as major drivers of $g_s$. Our analyses did detect an effect of VPD on $g_s$, but found that it was of secondary importance to plant functional type or species identity and shallow soil moisture. For several other meteorological variables, such as atmospheric $[CO_2]$ and shortwave radiation, however, the response of $g_s$ found here was less consistent with previous research. The data and model reported here, therefore, provide a perspective on landscape scale values and drivers of $g_s$ that differs from many laboratory-based approaches.

$G_s$ has been shown to increase with radiation[6] until a threshold of maximum $g_s$ is reached[35]. Here, both grasses and trees showed a hump-shaped pattern of $g_s$ with increasing shortwave radiation. For grasses, $g_s$ increased slightly with shortwave radiation until approximately 1100 $\mu$mol $m^{-2}$ $s^{-1}$ before decreasing. For woody plants, the threshold was lower at 500 $\mu$mol $m^{-2}$ $s^{-1}$. In this study, the effect of radiation on $g_s$ was assessed by averaging all other observed variable values across a range of radiation values. This should have allowed the detection of an increasing relationship between radiation and $g_s$, unless, under natural conditions, it is the case that some variables limited $g_s$ as radiation increased. It is likely, for example, that plants exhausted plant available water immediately around their roots by midday so that no naturally occurring $g_s$ values increase with radiation through the day[41]. This midday depression in $g_s$ has been documented in the field[39,42]. Where soils are consistently well-watered, $g_s$ may continue increasing as shortwave radiation increases[14] but consistently well-watered soils may only occur during heavy rains when shortwave radiation values do not reach high values. This hypothesis highlights both the strengths and weaknesses of the field data approach used in this study. Data from this study provide more realistic estimates of $g_s$ during the years and conditions of this study, but do not provide inference to conditions unlike those observed during the study (*i.e.*, extreme conditions associated with climate change).

$G_s$ also increased with atmospheric [$CO_2$]. This relationship is surprising, as previous studies have shown the opposite: $g_s$ decreased as ambient [$CO_2$] increased, presumably because plants could rapidly assimilate and close stomata to reduce water loss[7,14,41,43]. Other variables, like VPD and soil moisture, might mask the response of $g_s$ to atmospheric [$CO_2$]. Atmospheric [$CO_2$] was highest in the morning and decreased throughout the day (data not shown). Thus, atmospheric [$CO_2$] decreased as shortwave radiation and VPD were likely to increase and soil moisture likely to decrease. Because shallow soil moisture was a primary driver of $g_s$, it is likely that $g_s$ decreased as a result of water stress rather than decreasing [$CO_2$]. Regardless of the mechanism, our results suggest that the laboratory-based observations of [$CO_2$] effects on $g_s$ were overwhelmed by the effects of other environmental conditions.

To estimate how environmental variables affect $g_s$ on the landscape, $g_s$ was modeled for four sites that represented a broad range of abiotic conditions from fairly mesic to fairly xeric savanna[44] and clay to sand soils. $G_s$ was surprisingly similar among most sites, with the exception of the wet/sand site. $g_s$ was 14 % - 24 % and 66 % - 92 % greater in the wet/sand site than the other sites for grasses and woody plants, respectively. Also surprising was that soil type did not appear to have a consistent effect on $g_s$. The lack of a consistent response of $g_s$ to soil type suggests that model results are applicable across edaphic gradients. Again, results emphasize the importance of understanding soil moisture effects, but suggest that these soil moisture effects are consistently important across a wide range of soil types and plant species. This is important because it suggests that our models of $g_s$ may be applicable across a wide range of abiotic conditions.

This study highlights the difficulties of modeling $g_s$ at the landscape scale. Despite large sample sizes, the dataset was highly variable, and our models explained only a modest proportion of variance (25 % for grasses and 54 % for woody plants, respectively). Plant-to-plant variation was anticipated to have explained a large portion of the variation in the dataset[14]; however, averaging measurements over 2-hour increments provided nominal improvements (*i.e.*, <2 % of error; data not shown). This suggested that plant-to-plant variation explained little of the residual variance. Plant age was not included as a parameter in this study, but may have accounted for some of the unexplained variation[14,41]. A more likely source of variation is leaf-level environmental conditions. As stomatal aperture can change in response to leaf-level conditions, such as interstomatal [$CO_2$], leaf water potential, and leaf temperature, including these leaf-level parameters may be necessary to explain much of the unexplained variance in our dataset. Indeed, leaf-level models of $g_s$ that incorporate these types of parameters often explain upwards of 80% of variation in $g_s$[11].

Results provided novel insight into grass and woody plant rooting patterns in savannas. For nearly a century, Walter's two-layer hypothesis has suggested that grasses and trees can coexist because grasses use shallow soil moisture and trees use deep soil moisture[24,37,45]. Our results are consistent with recent finding$_s$ from hydrologic tracer experiments in Kruger Park that indicated that both grasses and trees rely on shallow soil water but that trees rely slightly more on deeper water than grasses[21,27]. More specifically, shallow water was found to be about 3.7 times more important in explaining variance in $g_s$ than deep water for grasses (Fig. 1). In contrast, shallow water was 2.1 times more important than deep water for woody plants. This suggested that both grasses and trees rely more on shallow than deep water but that grasses rely even more on shallow water than trees. Further, the fact that precipitation regime was more important to woody plants than grasses also supports the idea that woody plants rely more on deeper soil water than grasses. This is because wetter sites were more likely to realize deeper soil water penetration, which is likely to be more important to woody plants than grasses.

This study provides a prioritized list of variables important to landscape $g_s$ in this region. Results indicate that plant identity and shallow soil moisture are of greater importance than atmospheric conditions and several environmental drivers that are commonly included in models of $g_s$. Model performance decreased markedly when species was replaced with plant functional type as a predictor, and decreased even more when neither was included in the model. While incorporating species into a global circulation or land surface model may not be practical, it is possible to include plant functional type data and species-level data may be useful for increasing accuracy in canopy or ecosystem-level modeling.

REFERENCES

1. Beerling, D. J. & Beerling, D. J. Gas valves , forests and global change : a commentary on Jarvis ( 1976 ) ‘ The interpretation of the variations in leaf water potential and stomatal conductance found in canopies in the field ’. *Philos. Trans. R. Soc. B-Biological Sci.* (2015).

2. Lin, Y.-S. *et al.* Optimal stomatal behaviour around the world. *Nat. Clim. Chang.* 1–6 (2015). doi:10.1038/nclimate2550

3. Buckley, T. N. & Mott, K. a. Modelling stomatal conductance in response to environmental factors. *Plant, Cell Environ.* **36,** 1691–1699 (2013).

4. Ding, R. *et al.* A dynamic surface conductance to predict crop water use from partial to full canopy cover. *Agric. Water Manag.* **150,** 1–8 (2015).

5. Bonan, G. B., Williams, M., Fisher, R. a. & Oleson, K. W. Modeling stomatal conductance in the Earth system: linking leaf water-use efficiency and water transport along the soil-plant-atmosphere continuum. *Geosci. Model Dev. Discuss.* **7,** 3085–3159 (2014).

6. Hiyama, T., Kochi, K., Kobayashi, N. & Sirisampan, S. Seasonal variation in stomatal conductance and physiological factors observed in a secondary warm-temperate forest. *For. Ecosyst. Environ. Scaling Up from Shoot Modul. to Watershed* 97–110 (2005). doi:10.1007/4-431-29361-2_10

7. Alexandre, C., Carvalho, C. D. E., Silva, E. D. E. O. & Alves, M. Impact of climate change on plants, fruits, and grains. *Rev. Caatinga* **2125,** 205–212 (2014).

8. Gao, J. *et al.* Biophysical limits to responses of water flux to vapor pressure deficit in seven tree species with contrasting land use regimes. *Agric. For. Meteorol.* **200,** 258–269 (2015).

9. Jarvis, P. G. Interpretation of variations in leaf water potential and stomatal conductance found in canopies in field. *Philos. Trans. R. Soc. B-Biological Sci.* **273,** 593–610 (1976).

10. Ball, J. T., Woodrow, I. E. & Berry, J. A. A Model Predicting Stomatal Conductance and its Contribution to the Control of Photosynthesis under Different Environmental Conditions. *Prog. Photosynth. Res.* 221–224 (1987). doi:citeulike-article-id:8423355

11. Damour, G., Simonneau, T., Cochard, H. & Urban, L. An overview of models of stomatal conductance at the leaf level. *Plant, Cell Environ.* **33,** 1419–1438 (2010).

12. De Kauwe, M. G. *et al.* A test of an optimal stomatal conductance scheme within the CABLE land surface model. *Geosci. Model Dev.* **8,** 431–452 (2015).

13. Berry, J. a., Beerling, D. J. & Franks, P. J. Stomata: Key players in the earth system, past and present. *Curr. Opin. Plant Biol.* **13,** 233–240 (2010).

14. Jarvis, P. G. & Mansfield, T. A. *Stomatal Physiology*. (Cambridge University Press, 1981).

15. Cutler, D. R. *et al.* Random forests for classification in ecology. *Ecology* **88,** 2783–92 (2007).

16. Flexas, J. *et al.* Stomatal and mesophyll conductances to CO2 in different plant groups: Underrated factors for predicting leaf photosynthesis responses to climate change? *Plant Sci.* **226,** 41–48 (2014).

17. du Toit, J. T., Rogers, K. H. & Biggs, H. C. *The Kruger Experience*. (Island Press, 2003).

18. Buitenwerf, R., Kulmatiski, A. & Higgins, S. I. Soil water retention curves for the major soil types of the Kruger National Park. 1–9 doi:10.4102/koedoe.v56i1.1228

19. Kulmatiski, A., Beard, K. H., Verweij, R. J. T. & February, E. C. A depth-controlled tracer technique measures vertical, horizontal and temporal patterns of water use by trees and grasses in a subtropical savanna. *New Phytol.* **188,** 199–209 (2010).

20. Kulmatiski, A. & Beard, K. H. Woody plant encroachment facilitated by increased precipitation intensity. *Nat. Clim. Chang.* **3,** 833–837 (2013).

21. Mazzacavallo, M. G. & Kulmatiski, A. Modelling Water Uptake Provides a New Perspective on Grass and Tree Coexistence. *PLoS One* **10,** e0144300 (2015).

22. Kirkham, M. B. Horizontal root growth: Water uptake and stomatal resistance under microgravity. *VADOSE Zo. J.* **7,** 1125–1131 (2008).

23. *Plant Physiological Ecology: Field methods and instrumentation*. (Springer Netherlands, 1991).

24. February, E. C., Higgins, S. I., Bond, W. J. & Swemmer, L. Influence of competition and rainfall manipulation on the growth responses of savanna trees and grasses. *Ecology* **94,** 1155–1164 (2013).

25. *The ASCE Standardized Reference Evapotranspiration Equation*. (American Society of Civil Engineers, 2005).

26. Ramoelo, A. *et al.* Validation of Global Evapotranspiration Product (MOD16) using Flux Tower Data in the African Savanna, South Africa. *Remote Sens.* **6,** 7406–7423 (2014).

27. Kulmatiski, A. & Beard, K. H. Root niche partitioning among grasses, saplings, and trees measured using a tracer technique. *Oecologia* **171,** 25–37 (2013).

28. Fox, J. & Weisberg, S. An {R} companion to applied regression. *Thousand Oaks CA Sage* (2011). at <http://socserv.socsci.mcmaster.ca/jfox/Books/Companion>

29. Hothorn, T., Bretz, F. & Westfall, P. Simultaneous Inference in General Parametric Models. (2008).

30. Breiman, L. Random Forests. *Mach. Learn.* **45,** 5–32 (2001).

31. RStudio. (2015). at <http://www.rstudio.com/>

32. Ishwaran, H. & Kogalur, U. B. Random Forests for Survival, Regression and Classification (RF-SRC). (2015).

33. Ehrlinger, J. ggRandomForests: Visually Exploring Random Forests. (2015). at <http://cran.r-project.org/package=ggRandomForests>

34. Myers, J., Well, A. & Lorch, R. *Research Design and Statistical Analysis*. (Routledge, 2010).

35. Avissar, R., Avissar, P., Mahrer, Y. & Bravdo, B. A. A model to simulate response of plant stomata to environmental conditions. *Agric. For. Meteorol.* **34,** 21–29 (1985).

36. Kropp, H. & Ogle, K. Seasonal stomatal behavior of a common desert shrub and the influence of plant neighbors. *Oecologia* **177,** 345–355 (2014).

37. Gharun, M., Turnbull, T. L., Pfautsch, S. & Adams, M. a. Stomatal structure and physiology do not explain differences in water use among montane eucalypts. *Oecologia* 1171–1181 (2015). doi:10.1007/s00442-015-3252-3

38. Jolliet, O. & Bailey, B. . The effect of climate on tomato transpiration in greenhouses: measurements and models comparison. *Agric. For. Meteorol.* **58,** 43–62 (1992).

39. Collatz, G. J., Ball, J. T., Grivet, C. & Berry, J. a. Physiological and environmental regulation of stomatal conductance, photosynthesis and transpiration: a model that includes a laminar boundary layer. *Agric. For. Meteorol.* **54,** 107–136 (1991).

40. Long, S. P. & Ort, D. R. More than taking the heat: Crops and global change. *Curr. Opin. Plant Biol.* **13,** 241–248 (2010).

41. Willmer, C. & Fricker, M. *Stomata*. (Chapman & Hall, 1996).

42. Flexas, J. *et al.* Photosynthetic limitations in Mediterranean plants: A review. *Environ. Exp. Bot.* **103,** 12–23 (2014).

43. Jarvis, A. J., Mansfield, T. A. & Davies, W. J. Stomatal behaviour, photosynthesis and transpiration under rising CO2. *Plant, Cell Environ.* **22,** 639–648 (1999).

44. Sankaran, M. *et al.* Determinants of woody cover in African savannas. *Nature* **438,** 846–849 (2005).

45. Walter, H. *Vegetation of the Earth and Ecological Systems of the Geo-biosphere*. (Springer-Verlag, 1985).

APPENDICES

# Appendix A. SUPPLEMENTARY INFORMATION

Table A.1 Studied species and their respective common names, families, and growth forms.

| **Species** | **Common/Alt. Names** | **Family** | **Growth Form** |
|---|---|---|---|
| *Acacia nigrescenes* | Knobthorn | Fabaceae | Tree |
| *Acacia gerrardii* | Red thorn | Fabaceae | Tree |
| *Acacia tortilis* | Umbrella thorn | Fabaceae | Tree |
| *Albizia harveyi* | Common false thorn | Fabaceae | Tree |
| *Lonchocarpus capassa* | Apple-leaf | Fabaceae | Tree |
| *Aristida sp.* | | Poaceae | Grass |
| *Euclea crispa* | Blue guarri | Ebenaceae | Tree |
| *Bothriochloa radicans* | Stinking grass | Poaceae | Grass |
| *Cenchrus ciliaris* | Buffelgrass, African foxtail grass | Poaceae | Grass |
| *Loudetia simplex* | Common russet grass | Poaceae | Grass |
| *Tragus berteronianus* | Carrot seed grass | Poaceae | Grass |
| *Combretum apiculatum* | Red bushwillow | Combretaceae | Tree |
| *Combretum hereroense* | Russet bushwillow | Combretaceae | Tree |
| *Combretum imberbe* | Leadwood | Combretaceae | Tree |
| *Gymnosporia buxifolia* | Common spike thorn | Celastraceae | Tree |
| *Dichrostachys cinerea* | Sickle bush | Fabaceae | Shrub |
| *Phoenix reclinata* | Wild date palm | Arecaceae | Tree |
| *Enneapogon conchroides* | Nine-awned grass | Poaceae | Grass |
| *Euclea divinorum* | Magic guarri | Ebenaceae | Shrub/tree |
| *Lannea schwinfurthii* | False marula | Anacardiaceae | Tree |
| *Digitaria erianthra* | Common finger grass | Poaceae | Grass |
| *Grewia bicolour* | White raisin | Malvaceae | Tree |
| *Hyperthelia dissolute* | Yellow thatching grass | Poaceae | Grass |
| *Hyparrhenia filipendula* | | Poaceae | Grass |
| *Hyparrhenia hirta* | Common thatching grass | Poaceae | Grass |
| *Adenium multiflorum* | Impala lily | Apocynaceae | Forb |
| *Sclerocarya birrea* | Marula | Anacardiaceae | Tree |
| *Maerua angolensis* | Bead bean | Capparaceae | Tree |
| *Melinis repens* | Natal grass | Poaceae | Grass |
| *Strychnos madagascariensis* | Black monkey orange | Loganiaceae | Shrub/tree |
| *Colophospermum mopane* | Mopane | Fabaceae | Shrub/tree |
| *Panicum coloratum* | Small buffalo grass | Poaceae | Grass |
| *Panicum maximum* | Guinea grass | Poaceae | Grass |
| *Pogonarthria squarrosa* | Herringbone grass | Poaceae | Grass |

| | | | |
|---|---|---|---|
| *Ehretia rigida* | Sand paper bush | Boraginaceae | Tree |
| *Terminalia sericea* | Silver cluster-leaf | Combretaceae | Tree |
| *Heteropogon contortus* | Spear grass | Poaceae | Grass |
| *Setaria sphacelata* | Creeping bristle grass | Poaceae | Grass |
| *Themeda triandra* | Red oat grass | Poaceae | Grass |
| *Urochloa mosambicensis* | Bushveld signal grass | Poaceae | Grass |
| *Vangueria infausta* | Wild medlar | Rubiaceae | Shrub/tree |
| *Setaria incrassate* | Vlei bristle grass | Poaceae | Grass |
| *Securinega virosa* | White berry bush | Phyllanthaceae | Tree |
| *Ximenia caffra* | Sour plum | Olacaceae | Tree |
| *Dalbergia melanoxylon* | Zebra wood | Fabaceae | Tree |
| *Ziziphus mucronata* | Buffalo thorn | Rhamnaceae | Tree |

Table A.2 Mean observed daytime grass $g_s$ and summary statistics.

| **Site** | **Mean** | **SD** | **SE** |
|---|---|---|---|
| Dry/Clay | 66.92703 | 48.31501 | 2.178209 |
| Dry/Sand | 65.20629 | 38.89313 | 3.084426 |
| Wet/Sand | 62.27551 | 47.17955 | 1.939068 |
| Wet/Clay | 95.97528 | 79.05191 | 3.408170 |

Table A.3 Mean observed daytime woody plant $g_s$ and summary statistics.

| **Site** | **Mean** | **SD** | **SE** |
|---|---|---|---|
| Dry/Clay | 123.4944 | 71.23182 | 2.433232 |
| Dry/Sand | 128.6277 | 78.24701 | 3.105138 |
| Wet/Sand | 150.4774 | 116.4686 | 2.742905 |
| Wet/Clay | 197.6815 | 136.1406 | 3.939902 |

Table A.4 Mean modeled daytime grass $g_s$ and summary statistics.

| Site | Mean | SD | SE |
|---|---|---|---|
| Dry/Clay | 62.4447 | 17.33135 | 0.090633 |
| Dry/Sand | 64.82193 | 17.79558 | 0.092633 |
| Wet/Sand | 77.50184 | 15.41926 | 0.085978 |
| Wet/Clay | 67.82299 | 18.4539 | 0.134779 |

Table A.5 Mean modeled daytime woody plant $g_s$ and summary statistics.

| Site | Mean | SD | SE |
|---|---|---|---|
| Dry/Clay | 131.2803 | 31.64087 | 0.202651 |
| Dry/Sand | 134.822 | 35.12521 | 0.111966 |
| Wet/Sand | 252.5363 | 56.23957 | 0.313591 |
| Wet/Clay | 152.4924 | 46.67333 | 0.241039 |

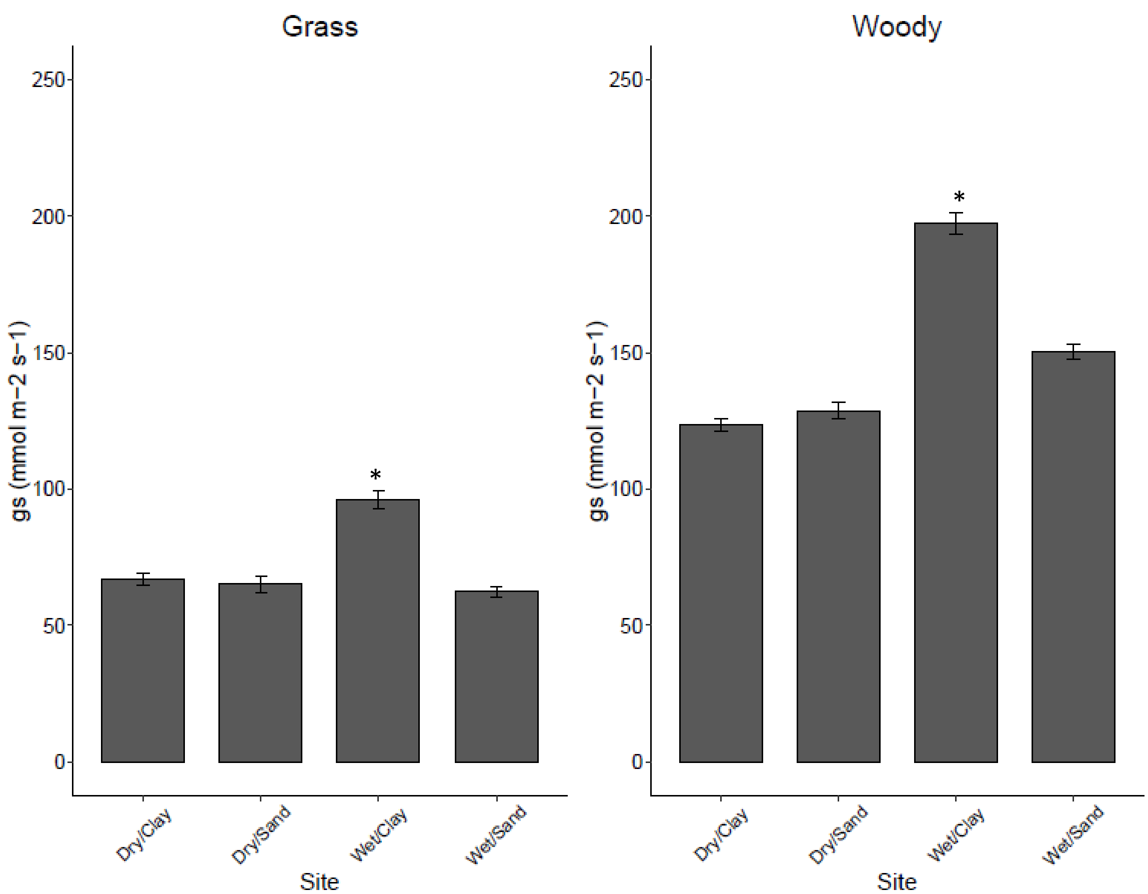


Fig. A1 Mean observed daytime gs for Kruger National Park and each study site. Error bars represent standard error. Asterisks indicate significance ($p<0.05$).

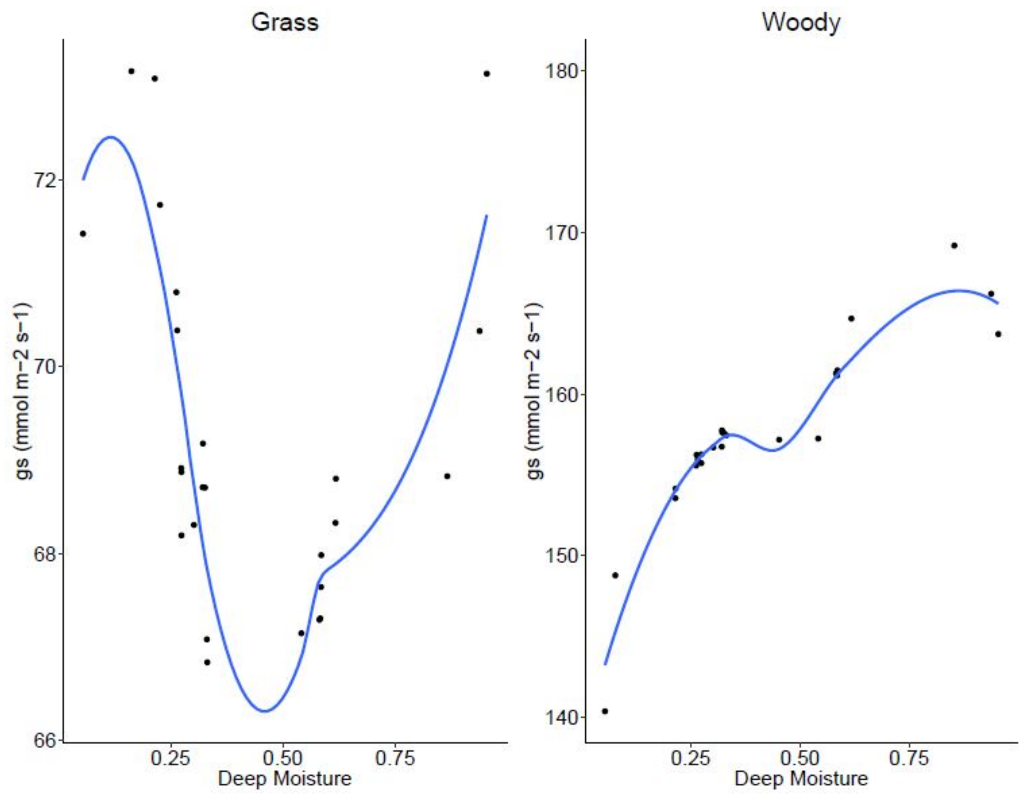


Fig A.2 Partial dependence plots for deep soil moisture for grasses and woody plants. The panels show predicted grass and woody plant gs as a function of deep soil moisture.

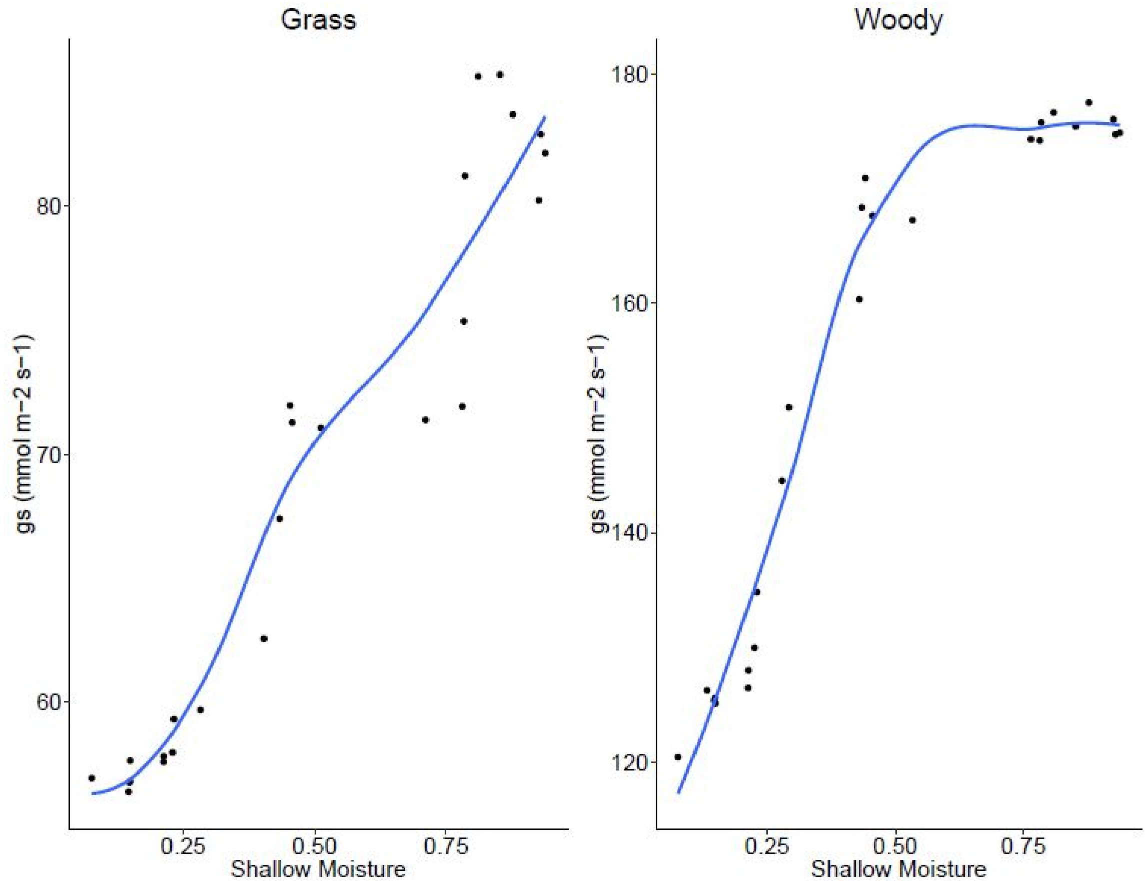


Fig A.3 Partial dependence plots for shallow soil moisture for grasses and woody plants. The panels show predicted grass and woody plant $g_s$ as a function of shallow soil moisture.

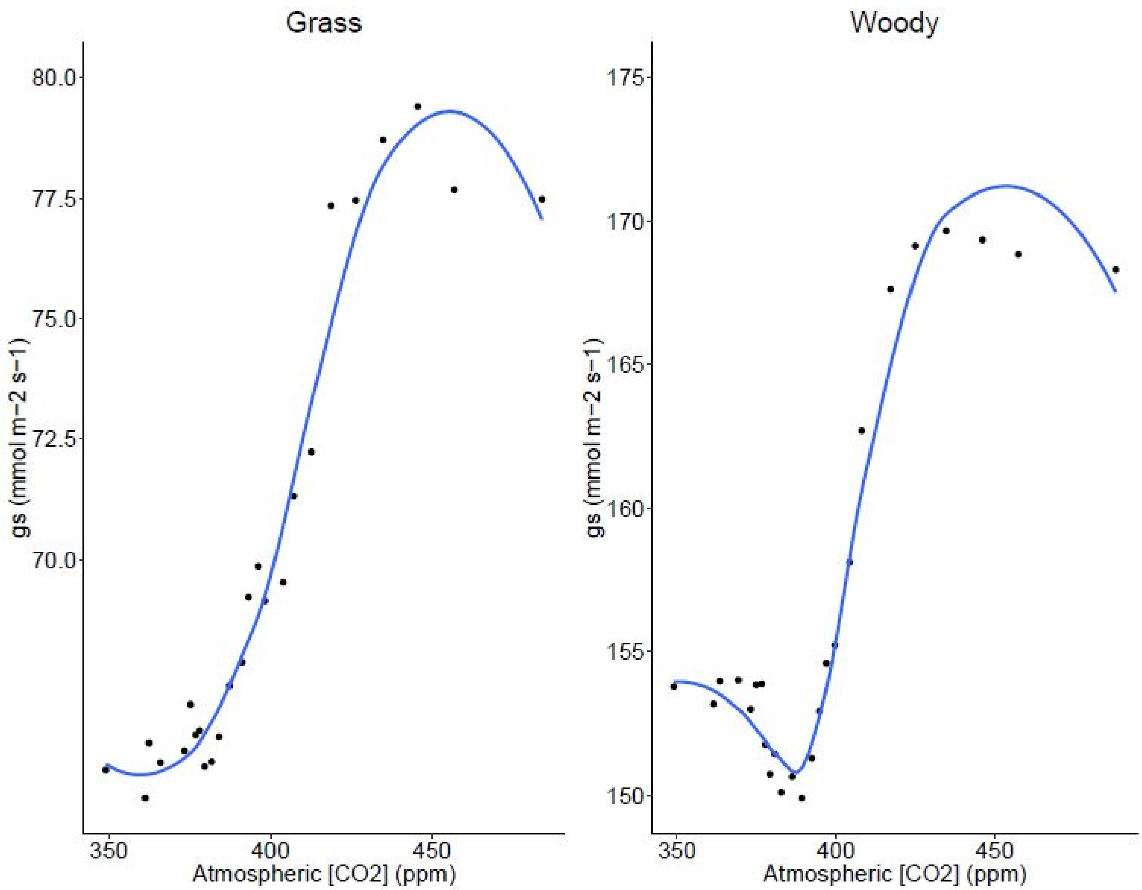


Fig A.4 Partial dependence plots for atmospheric [$CO_2$] for grasses and woody plants. The panels show predicted grass and woody plant $g_s$ as a function of atmospheric [$CO_2$].

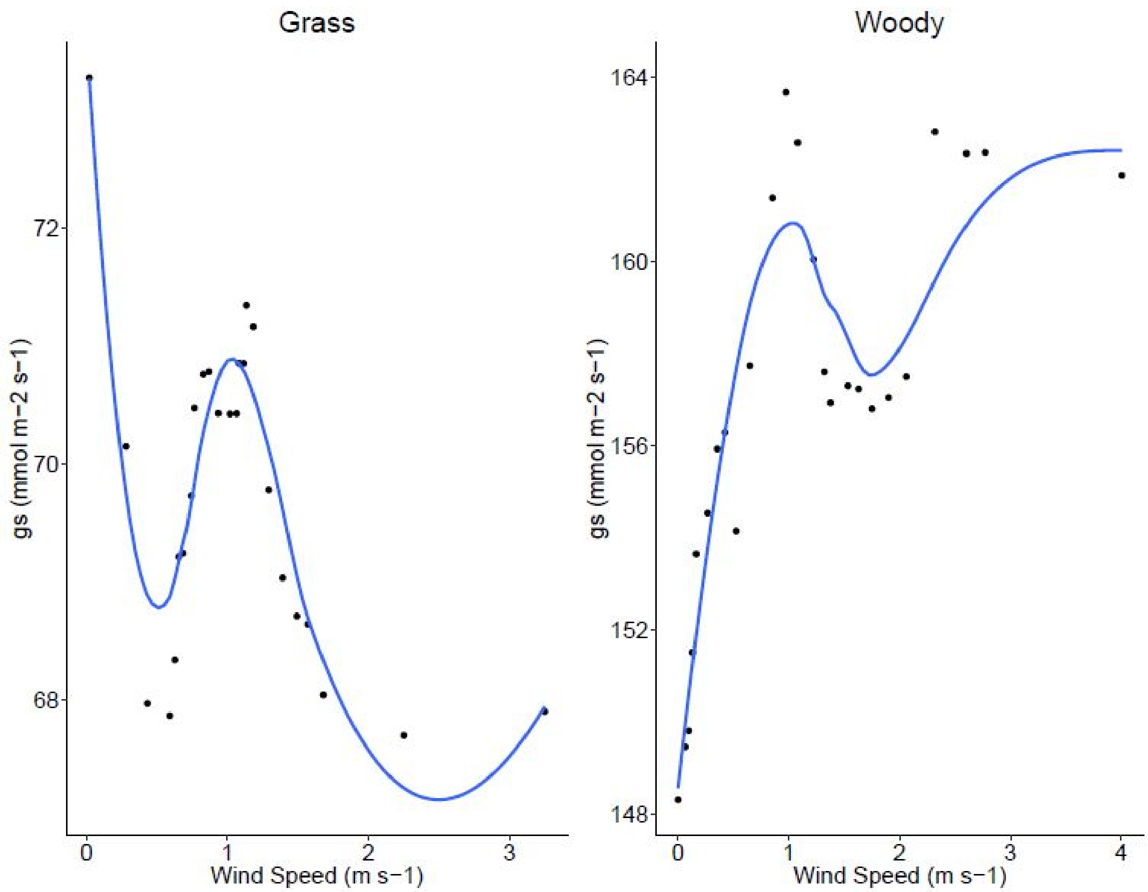


Fig A.5 Partial dependence plots for wind speed for grasses and woody plants. The panels show predicted grass and woody plant $g_s$ as a function of wind speed.

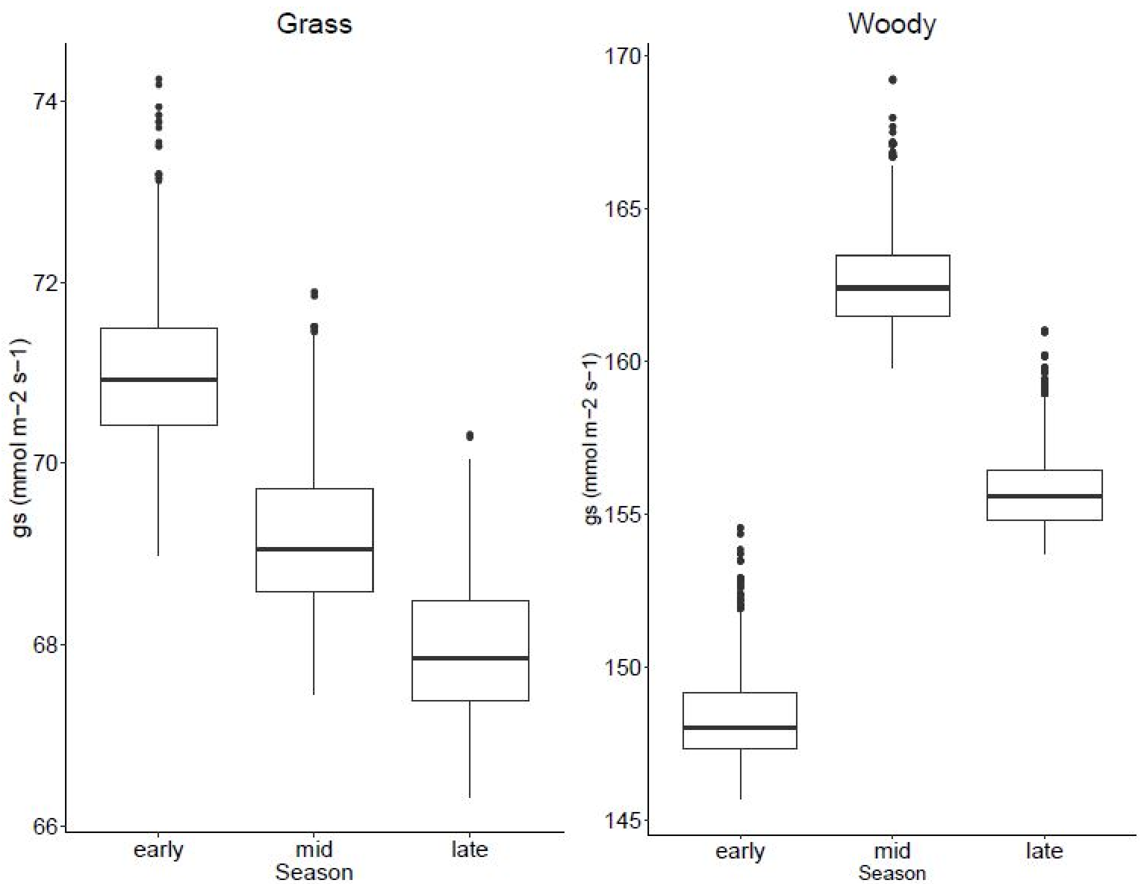


Fig A.6 Partial dependence plots for time of season for grasses and woody plants. The panels show predicted grass and woody plant $g_s$ as a function of time of season.

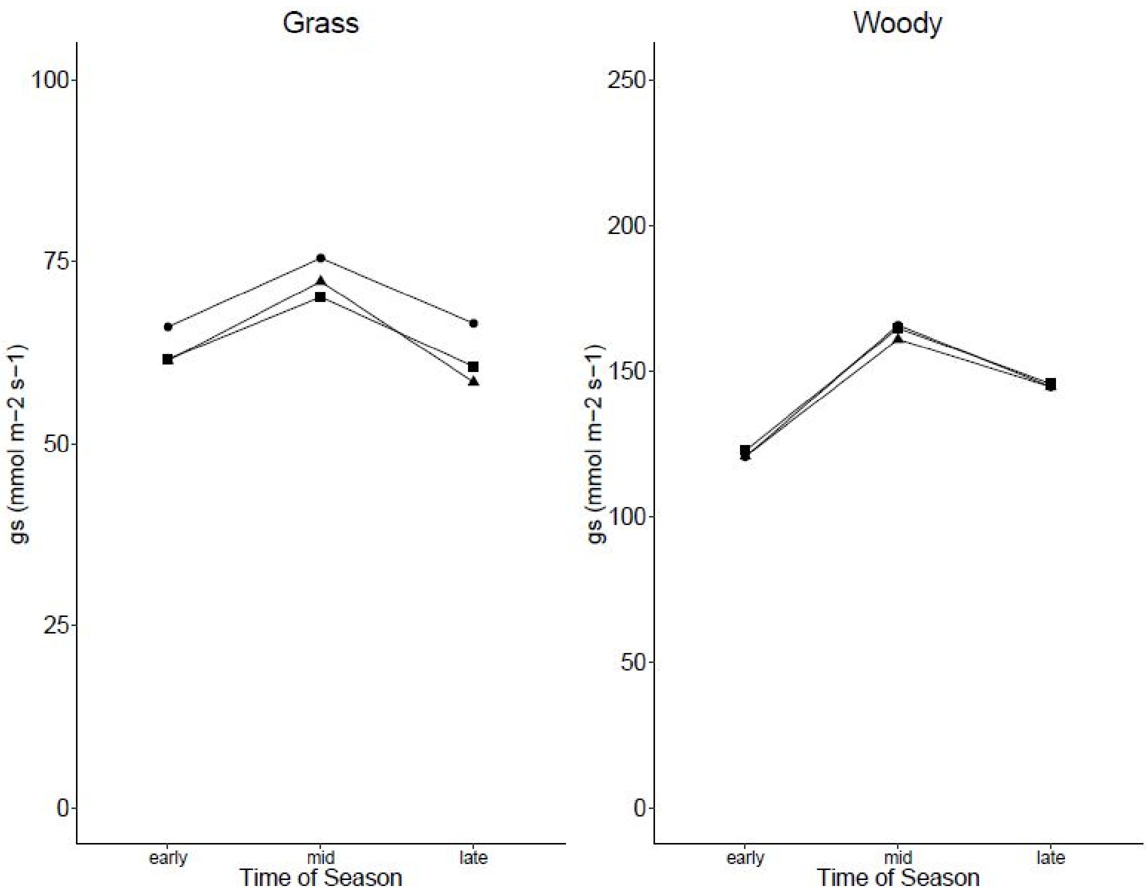


Fig A.7 Modeled seasonal gs for grasses and woody plants at the dry/sand site. The shape of the points indicates the species. In the grass panel: circles for Bothriochloa radicans, triangles for Panicum spp., and squares for Urochloa mosambicensis. In the woody panel: circles for *Acacia nigrescens*, triangles for *Dichrostachys cinerea*, and squares for *Securinega virosa*. Model predictions were averaged for each season and midday values are shown.

# Appendix B. STATISTICAL RESULTS

Table B.1 One-way analysis of variance (Type III) of observed mean daytime grass gs values from each study site. See Table 1 for a description of each site.

| Source | Sum of Squares | Mean Square | dF | F | p |
|---|---|---|---|---|---|
| Site | 49.8 | 16.602 | 3 | 28.399 | <0.001 |
| Error | 1104.3 | 0.585 | 1889 | | |
| Total | 1154.1 | 17.187 | 1892 | | |

Table B.2 One-way analysis of variance (Type III) of observed mean daytime woody plant gs values from each study site. See Table 1 for a description of each site.

| Source | Sum of Squares | Mean Square | dF | F | p |
|---|---|---|---|---|---|
| Site | 179.6 | 59.87 | 3 | 77.298 | <0.001 |
| Error | 3472.8 | 0.77 | 4484 | | |
| Total | 3652.4 | 60.64 | 4487 | | |

Table B.3 Tukey test for pairwise comparisons of mean observed daytime gs values for grasses by site. See Table 1 for a description of wet, dry, sand, and clay.

| Comparison | Estimate | SE | t-statistic | p |
|---|---|---|---|---|
| Dry/Sand – Dry/Clay | 0.019 | 0.046 | 0.406 | 0.977 |
| Wet/Sand – Dry/Clay | 0.009 | 0.037 | 0.246 | 0.995 |
| Wet/Clay – Dry/Clay | 0.461 | 0.039 | 11.698 | <0.001 |
| Wet/Sand – Dry/Sand | -0.010 | 0.041 | -0.239 | 0.995 |
| Wet/Clay – Dry/Sand | 0.442 | 0.043 | 10.234 | <0.001 |
| Wet/Clay – Wet/Sand | 0.452 | 0.033 | 13.768 | <0.001 |

Table B.4 Tukey test for pairwise comparisons of mean observed daytime gs values for woody plants by site. See Table 1 for a description of wet, dry, sand, and clay.

| Comparison | Estimate | SE | t-statistic | p |
|---|---|---|---|---|
| Dry/Sand – Dry/Clay | 0.075 | 0.070 | 1.074 | 0.699 |
| Wet/Sand – Dry/Clay | -0.036 | 0.045 | -0.802 | 0.849 |
| Wet/Clay – Dry/Clay | 0.344 | 0.048 | 7.209 | <0.001 |
| Wet/Sand – Dry/Sand | -0.111 | 0.067 | -1.652 | 0.341 |
| Wet/Clay – Dry/Sand | 0.269 | 0.069 | 3.894 | <0.001 |
| Wet/Clay – Wet/Sand | 0.380 | 0.044 | 8.669 | <0.001 |